# A New AVO Attribute for Hydrocarbon Prediction and Application to the Marmousi II Dataset*

**Changcheng Liu[1] and Prasad Ghosh[2]**

Search and Discovery Article #41764 (2016)
Posted January 25, 2016

*Adapted from extended abstract prepared in conjunction with oral presentation at AAPG/SEG International Conference & Exhibition, Melbourne, Australia, September 13-16, 2015, AAPG/SEG © 2016.

[1]Centre of Seismic Imaging, Geoscience Department, Universiti Teknologi PETRONAS, Ipoh, Malaysia (lccgreatwall@gmail.com)
[2]Centre of Seismic Imaging, Geoscience Department, Universiti Teknologi PETRONAS, Ipoh, Malaysia

## Abstract

At present, quantitative AVO plays a significant role in hydrocarbon prediction in many basins. Hydrocarbon prediction from seismic amplitude and AVO is a daunting task. Many AVO attributes are presented for this purpose. Based on the Mudrock equation, Smith and Gidlow (1987) defined an attribute named fluid factor as: $\Delta F=\Delta V_p/V_p-1.16\Delta V_s/V_s/\gamma$ (1) Where $\gamma$ is the background $V_p/V_s$ ratio, the constant 1.16 can be local value of $V_p$-$V_s$ relation. Fatti et al. (1994) redefined the fluid factor as: $\Delta F=R_p-1.16R_s/\gamma$ (2) Where $R_p$ is P-reflectivity and $R_s$ is S-reflectivity. However, there exist several pitfalls in the AVO technique. One of the pitfalls is that a high porosity and good quality brine sand can give a rising AVO response. In this paper, we propose a new attribute called "J" for hydrocarbon prediction as follow: $J=J_p \sin\alpha-J_s \cos\alpha$ (3) Numerical and Marmousi II model are used to test the new method in this paper. In the numerical simulation, brine responses of J attribute are relatively stable with varying of porosity whereas hydrocarbon responses decrease under effect of porosity. In these two fluid factor cases, water response with high porosity can equal to hydrocarbon response with lower porosity which cause an ambiguity in interpretation. A part of Marmousi II model is used to compare performances of different attributes. The results show that all three attribute can detect hydrocarbon sands. However, Smith and Gidlow's and Fatti's fluid factor also show anomalies for water-bearing layer which can be misleading whereas J attribute is more sensitive to hydrocarbon. J attribute is less ambiguous in hydrocarbon detection. In summary, this study presents a new AVO attribute J and we compare it with Smith and Gidlow's and Fatti's fluid factor. This method is simple, fast, and an effective exploration tool. Through Marmousi II model study, we demonstrated that J attribute can detect hydrocarbons and has fewer anomalies from a non-pay zone. In this case, J attribute has better performance than both Smith and Gidlow's and Fatti's fluid factor in hydrocarbon prediction. It can predict presence of possible hydrocarbon sand effectively and reduce the ambiguity caused by lithology. Further, AVO attribute has to be interpreted as a guideline in exploration. Predicting hydrocarbon from amplitude has to be geologically/rock physics considered with structure and petroleum system playing a major role in reducing exploration risk.

## Introduction

AVO interpretation for hydrocarbon prediction is a daunting task because pore-fill fluid and porosity affect amplitude simultaneously. A useful AVO attribute called "fluid factor" is presented for hydrocarbon prediction by Smith and Gidlow (1987) and Fatti et al. (1994) respectively. This study defines a new attribute "J" to detect hydrocarbons. It is supposed to be more sensitive to the existence of hydrocarbons and has less ambiguity caused by porosity. Numerical simulation and Marmousi II dataset are used to test the new attribute "J" and the results illustrate the effectiveness and less ambiguity of the J attribute. J attribute is a useful tool for hydrocarbon prediction and risk reduction in exploration.

At present, AVO attribute analysis plays a significant role in hydrocarbon prediction in many basins where rocks are generally soft, unconsolidated and are sensitive to fluid replacement and response as per Gassmann (Ghosh et al., 2014). However, there exist several pitfalls in amplitude interpretation. One of the pitfalls is that good quality brine sands can give rising AVO responses in line with Gassmann fluid replacement algorithm as shown in Figure 1 (Ghosh et al., 2010).

One of the widely-used AVO attributes for hydrocarbon prediction is fluid factor. Smith and Gidlow 1987 defined an attribute named fluid factor based on the Mudrock line (Castagna et al., 1985). The fluid factor is written as:

$$\Delta F = \frac{\Delta V_p}{V_p} - 1.16\frac{\Delta V_s}{V_s}/\gamma \qquad (1)$$

where, $\gamma$ is the background $V_p/V_s$ ratio and the constant 1.16 can be a local value of Mudrock line.

Fatti et al., 1994 redefined the fluid factor as:

$$\Delta F = R_p - 1.16R_s/\gamma \qquad (2)$$

where, $R_p$ is P-reflectivity and $R_s$ is S-reflectivity.

When the layers above and below the given interface are wet sand or shale, ΔF equals zero as the relationship of P-velocity (P-reflectivity) and S-velocity (S-reflectivity) fits the Mudrock line. When the layers are gas sand and shale, the difference increases as the calculated P-velocity contrast (P-reflectivity) is greater than the actual P-velocity contrast (P-reflectivity) and ΔF decreases away from zero. Thus, ΔF creates a display which highlights the presence of hydrocarbon. Note that for different basins, the constant in the above equations need an adjustment.

## Development of New Algorithm

We now propose a new attribute called "J" to predict the existence of hydrocarbon. It will be demonstrated that it is more stable and less ambiguous by the incorporation of rock physics constraint. It is defined as:

$$J = J_p sin\alpha - J_s cos\alpha \quad (3)$$

where,

$$J_p = 2\left(\frac{\Delta\rho}{\rho} + 2\frac{\Delta V_p}{V_p}\right)/\gamma^2 \quad (4)$$

$$J_s = 2\left(\frac{\Delta\rho}{\rho} + 2\frac{\Delta V_s}{V_s}\right)/\frac{V_p^2}{V_s^2} \quad (5)$$

$\gamma$ is the $V_p/V_s$ ratio for the interface of brine sand and shale, and $\alpha$ is the rotation angle defined as the angle between Y-axis parallel line and brine response in the $J_p$-$J_s$ curve which is based on rock parameters extracted from the reservoir and surrounding layer.

$J_s$ is a part of the AVO gradient according to Shuey's approximation (Shuey, 1985). $J_p$ is derived from density, $V_p$ and $\gamma$ as shown in Equation 4. When the layers are hydrocarbon sand and shale, $J_p$ decreases whereas $J_s$ increases. Then the response of hydrocarbon sand moves from background trend.

Through the Biot-Gassmann theory, we calculate $V_p$, $V_s$ and density and derive $J_p$ and $J_s$ in different porosity and water saturation cases with extracted rock physics parameters. As rotation of the coordinate is based on the response of wet sand, the brine response of J is close to zero whereas the hydrocarbon response of J is more negative. Thus, J is supposed to be sensitive to fluid.

## Numerical Simulation

A numerical simulation is built up for attributes application and comparison. The model has two layers: top layer is shale; bottom layer is pure quartz sand. Rock physics parameters are shown in Table 1 (Data from Avseth et al., 2005; Fjar et al., 2008; and Zhu, 2012). There is no extra porosity and fluid effects to be considered in the shale layer. For the sand layer, porosity and hydrocarbon saturation are calculated into the model. The range of porosity is from 5% to 35% and the range of hydrocarbon saturation is from 0% to 100%.

Matrix rock parameters are calculated in different porosity cases according to the Biot-Gassmann theory. $J_p$ and $J_s$ are derived from $V_p$, $V_s$ and density of brine, oil, gas sands, and shale. The differences among gas, oil, and wet sand are shown in Figure 2. In Figure 2 (left), both $J_p$ and $J_s$ can distinguish different fluid type for each porosity case. The hydrocarbon response of $J_p$ is closer to zero than the brine response of $J_p$ whereas the hydrocarbon response of $J_s$ is more positive than the brine response of $J_s$. However, the difference is not obvious enough to be a hydrocarbon indicator.

Figure 2 (right) shows J which is computed after a counter-clockwise coordinate rotation with the angle $\alpha$. In this model, the rotation angle is 55.9 degrees. The background $V_p/V_s$ ratio is 1.83 which is the arithmetic mean of $V_p/V_s$ ratios in brine sand with different porosity cases. We can see responses of brine and hydrocarbons are distinguished clearly after rotation. Although gas and oil sand responses are possible to be

misinterpreted with varying porosity, brine sand responses show stable and no mixture with hydrocarbon cases. J attribute works well in hydrocarbon prediction that brine and hydrocarbon can be distinguished clearly by the dash line in the Figure 2 (right). Brine responses spread on the right side of this line whereas hydrocarbon responses spread on the left side.

Further, we compare J attribute with two fluid factors presented by Smith & Gidlow (1987) and Fatti et al. (1994). The results are given by Figure 3. Brine and hydrocarbon responses of J attribute can be separated clearly by the dash line shown in Figure 3 (left). The plots above the dash line are brine responses and the plots below this line present hydrocarbon. Brine responses are stable irrespective of porosity whereas hydrocarbon responses decrease under effect of porosity. It illustrates that J attribute reduces the ambiguity caused by good quality wet sand.

As a comparison, results of two fluid factors are given in Figure 3 (middle) and (right) respectively. Though brine and hydrocarbon sands can be separated in each porosity case, water response with high porosity can be equal to hydrocarbon response with lower porosity which cause the ambiguity in interpretation in these two fluid factor cases. If we set a line (shown as dash lines in Figure 3 middle and right) to distinguish water and hydrocarbon, only hydrocarbon responses with larger porosity will be not misinterpreted with brine responses.

## Application

The Marmousi II model (Martin et al., 2006) shown in Figure 4 is used to compare the performances of different attributes in this study. Only a part marked with a blue frame is selected, which has a relatively stable $V_p/V_s$ ratio ($V_p/V_s$ ratio is observed to be around 2.3). In this area, it contains four gas reservoirs and two oil reservoirs. All attributes are derived from the given rock property parameters in this model set and the rotation angle of the J attribute is estimated from the above numerical simulation.

Results of J attribute, Smith and Gidlow's fluid factor and Fatti's fluid factor are given in Figure 5 (A) (B) and (C) respectively. It can be found that all three attributes can detect hydrocarbon sands. However, Smith and Gidlow's and Fatti's fluid factor also show anomalies marked by blue arrows for water-bear layers shown in Figure 5 (B) and (C). Those anomalies can be misinterpreted as hydrocarbons. J attribute is more sensitive to hydrocarbon. Comparing J with these two fluid factors, J attribute is less ambiguous in hydrocarbon prediction in this case.

## Conclusion

This study presents a new AVO attribute "J" and compares it with Smith and Gidlow's and Fatti's fluid factor. Through numerical simulation and application on Marmousi II model, J attribute demonstrates the ability of hydrocarbon prediction and has fewer anomalies from non-pay zone. In this case, J attribute has a better performance than both Smith and Gidlow's and Fatti's fluid factor in hydrocarbon prediction. J attribute can predict presence of possible hydrocarbon sand effectively and reduce exploration risk.

## Acknowledgement

The authors gratefully acknowledge all members in the Centre of Seismic Imaging for their valued comments. We would also like to thank PETRONAS for their support to this study.

## References Cited


Avseth, P., T. Mukerji, and G. Mavko, 2005, Quantitative Seismic Interpretation: Applying Rock Physics Tools to Reduce Interpretation Risk: Cambridge University Press, New York, 359 p.

Biot, M.A., 1956, Theory of Propagation of Elastic Waves in a Fluid-Saturated Porous Solid. II. Higher Frequency Range: The Journal of the Acoustical Society of America, v. 28/2, p. 179-191.

Castagna, J.P., M.L. Batzle, and R.L. Eastwood, 1985, Relationships between Compressional-Wave and Shear-Wave Velocities in Clastic Silicate Rocks: Geophysics, v. 50/4, p. 571-581.

Fatti, J.L., G.C. Smith, P.J. Vail, P.J. Strauss, and P.R. Levitt, 1994, Detection of Gas in Sandstone Reservoirs Using AVO Analysis: A 3-D Seismic Case History Using the Geostack Technique: Geophysics, v. 59/9, p. 1362-1376.

Fjar, E., R.M. Holt, A.M. Raaen, R. Risnes, and P. Horsrud, 2008, Petroleum Related Rock Mechanics 2nd ed.: Developments in Petroleum Science 53, Elsevier, Amsterdam, Netherlands, 491 p.

Gassmann, F., 1961, Uber die elastizitat poroser Medien. Vier. der Natur. Gesellschaft in Zurich, v. 96, p. 1-23.

Ghosh, D., M.F.A. Halim, M. Brewer, B. Viratno, and N. Darman, 2010, Geophysical Issues and Challenges in Malay and Adjacent Basins from an E & P Perspective: The Leading Edge, v. 29/4, p. 436-449.

Ghosh, D., M. Sajid, N.A. Ibrahim, and B. Viratno, 2014, Seismic Attributes Add a New Dimension to Prospect Evaluation and Geomorphology Offshore Malaysia: The Leading Edge, v. 33/5, p. 536-545.

Martin, G.S., R. Wiley, and K.J. Marfurt, 2006, Marmousi II: An Elastic Upgrade for Marmousi: The Leading Edge, v. 25/2, p. 156-166.

Shuey, R.T., 1985, A Simplification of the Zoeppritz Equations: Geophysics, v. 50/4, p. 609-614.

Smith, G.C., and P.M. Gidlow, 1987, Weighted Stacking for Rock Property Estimation and Detection of Gas: Geophysical Prospecting, v. 35/9, p. 993-1014

Zhu, T., 2012, Some Useful Numbers on the Engineering Properties of Materials, for Geology 615 at Stanford University, Department of Geophysics.

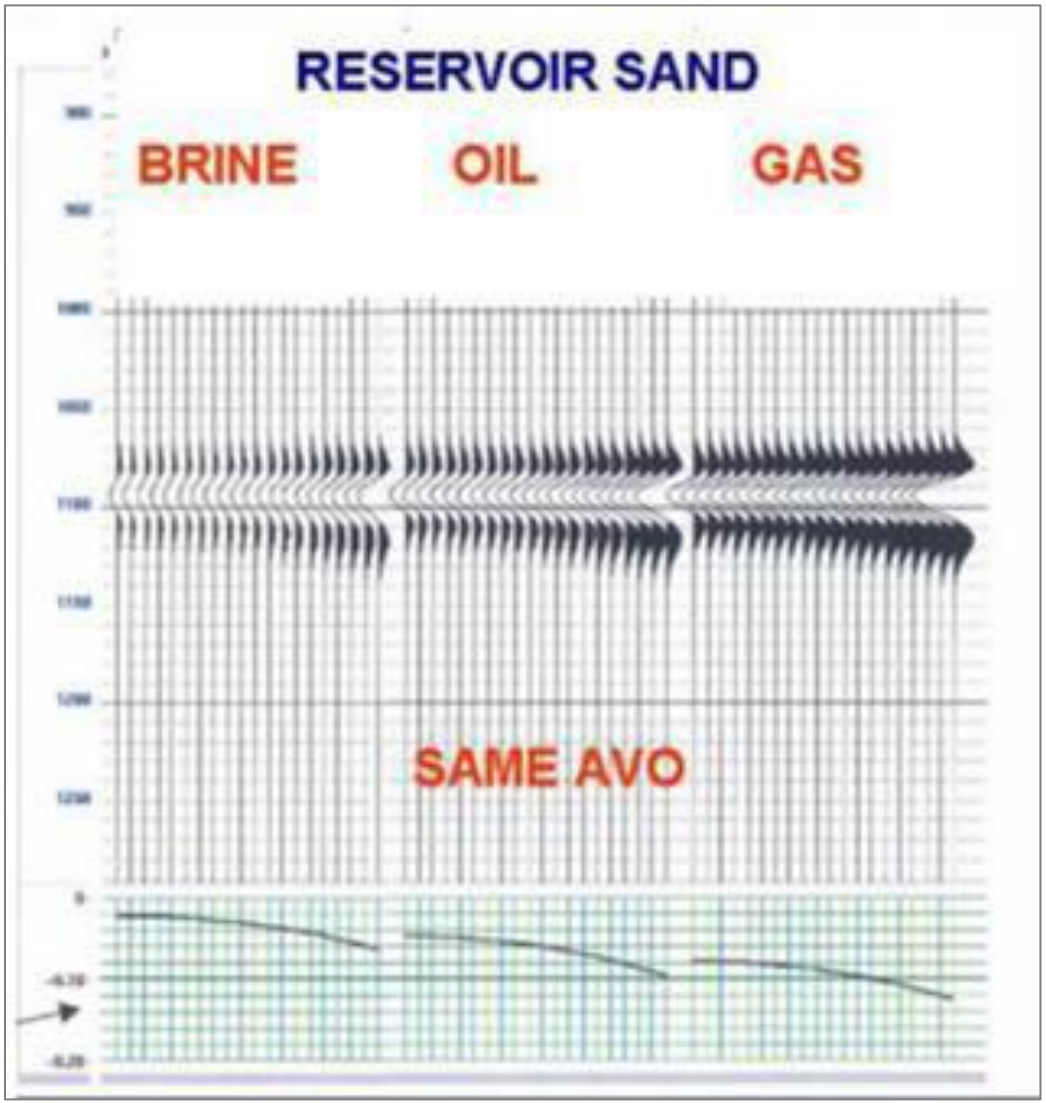


Figure 1. Different fluid types give similar rising AVO responses. (Ghosh et al., 2010).

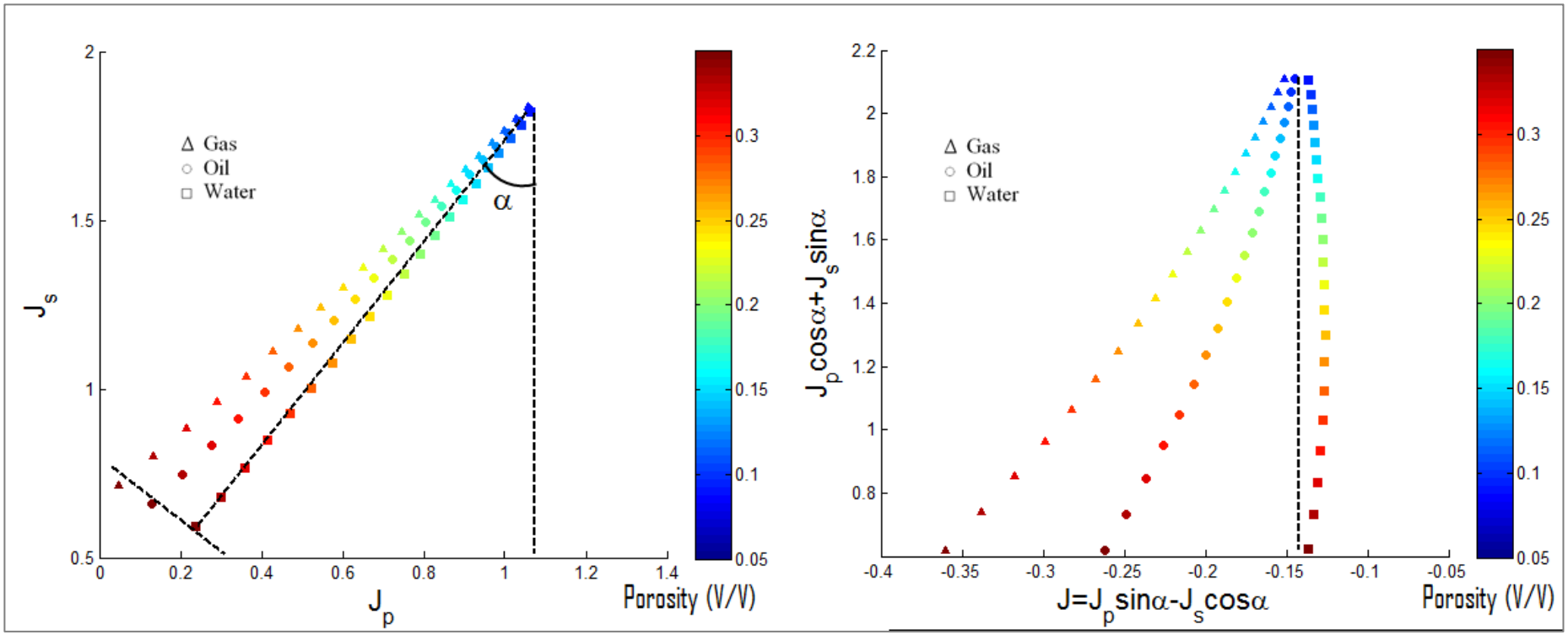


Figure 2. (left) Cross plot of brine (square), oil (circle), and gas (triangle) responses where X-axis is $J_p$, Y-axis is $J_s$. (right) Responses brine (square), oil (circle), and gas (triangle) situation after coordinate rotation. All rock fluid in this figure is single phase. The colour bar shows porosity.

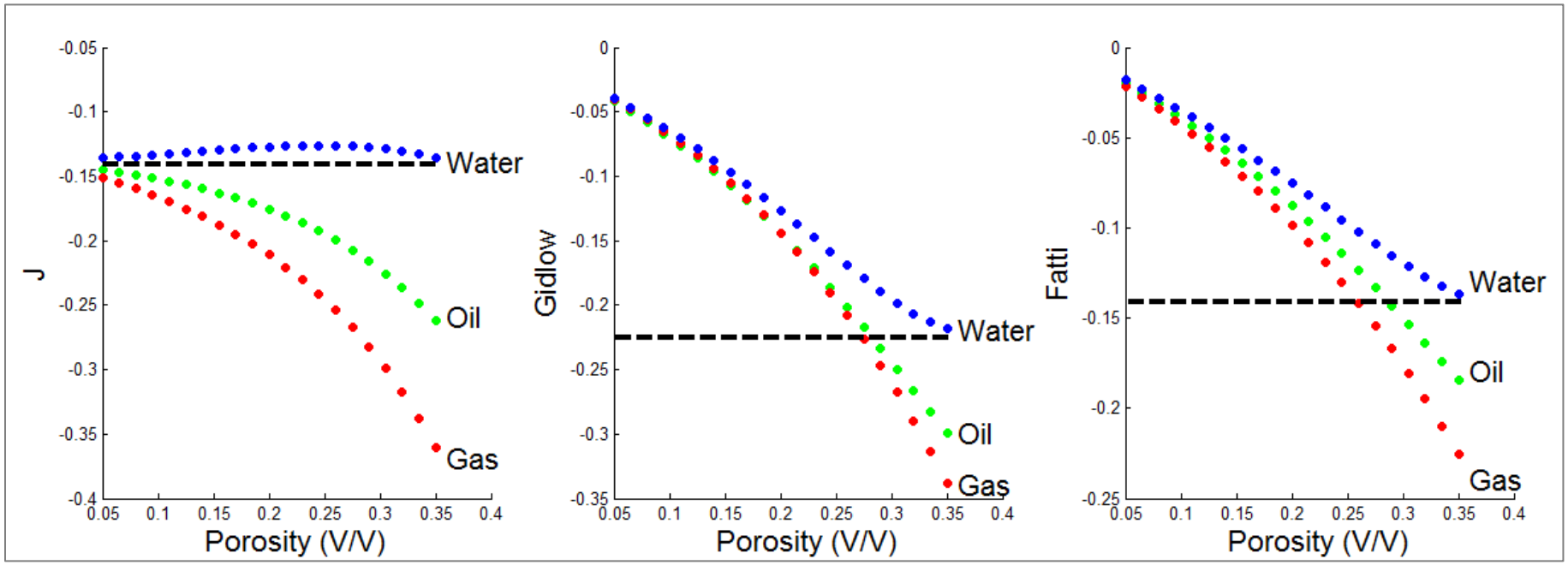


Figure 3. Cross plot of porosity versus attributes: (left) J attribute, (middle) Fluid factor by Smith and Gidlow, (right) Fluid factor by Fatti. All rock fluid in this figure is single phase. Note that the J attribute can distinguish the fluid irrespective of porosity compared to other attributes.

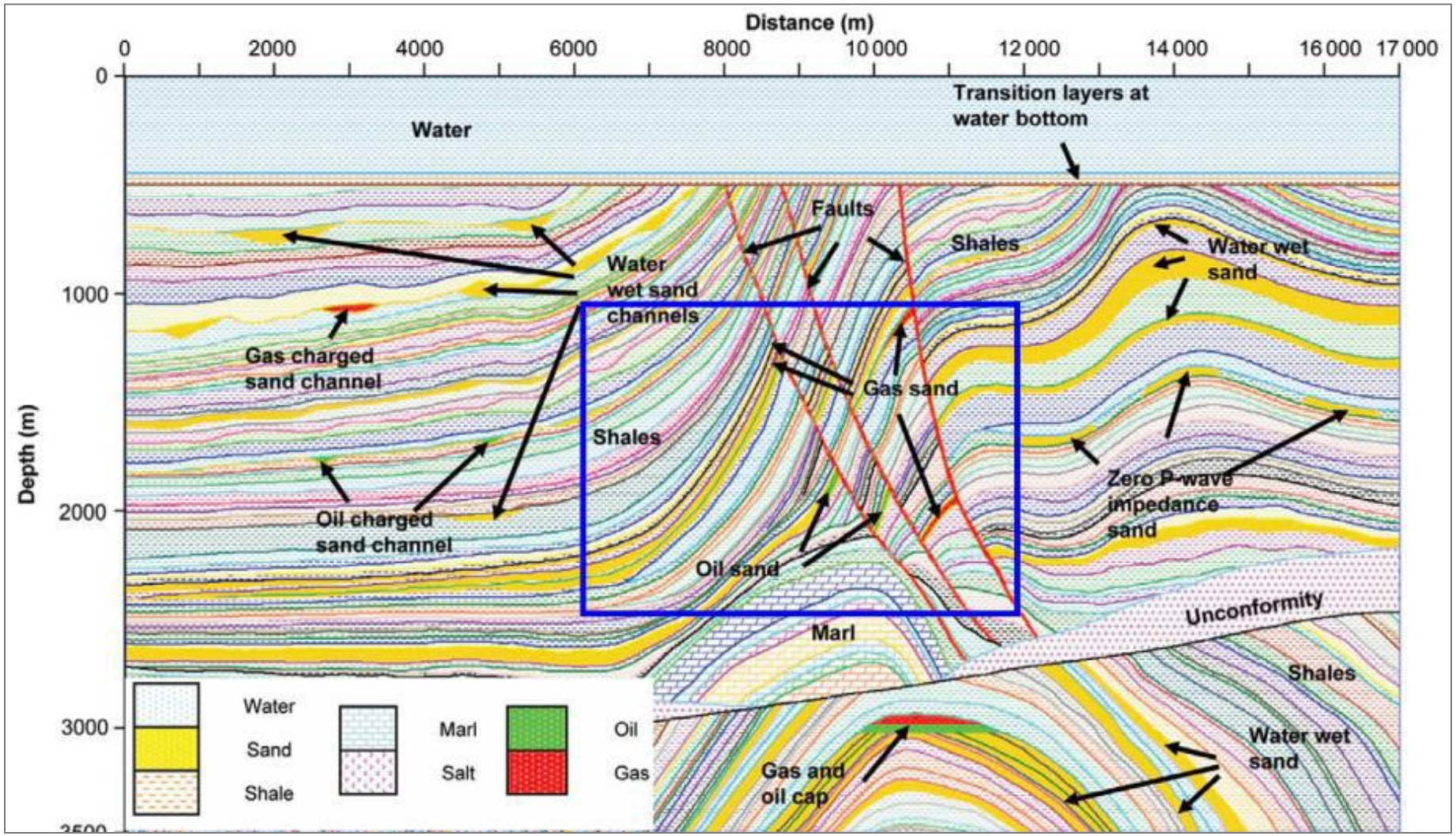


Figure 4. Marmousi II model, structural elements, horizons, and lithologies. (Martin et al., 2006).

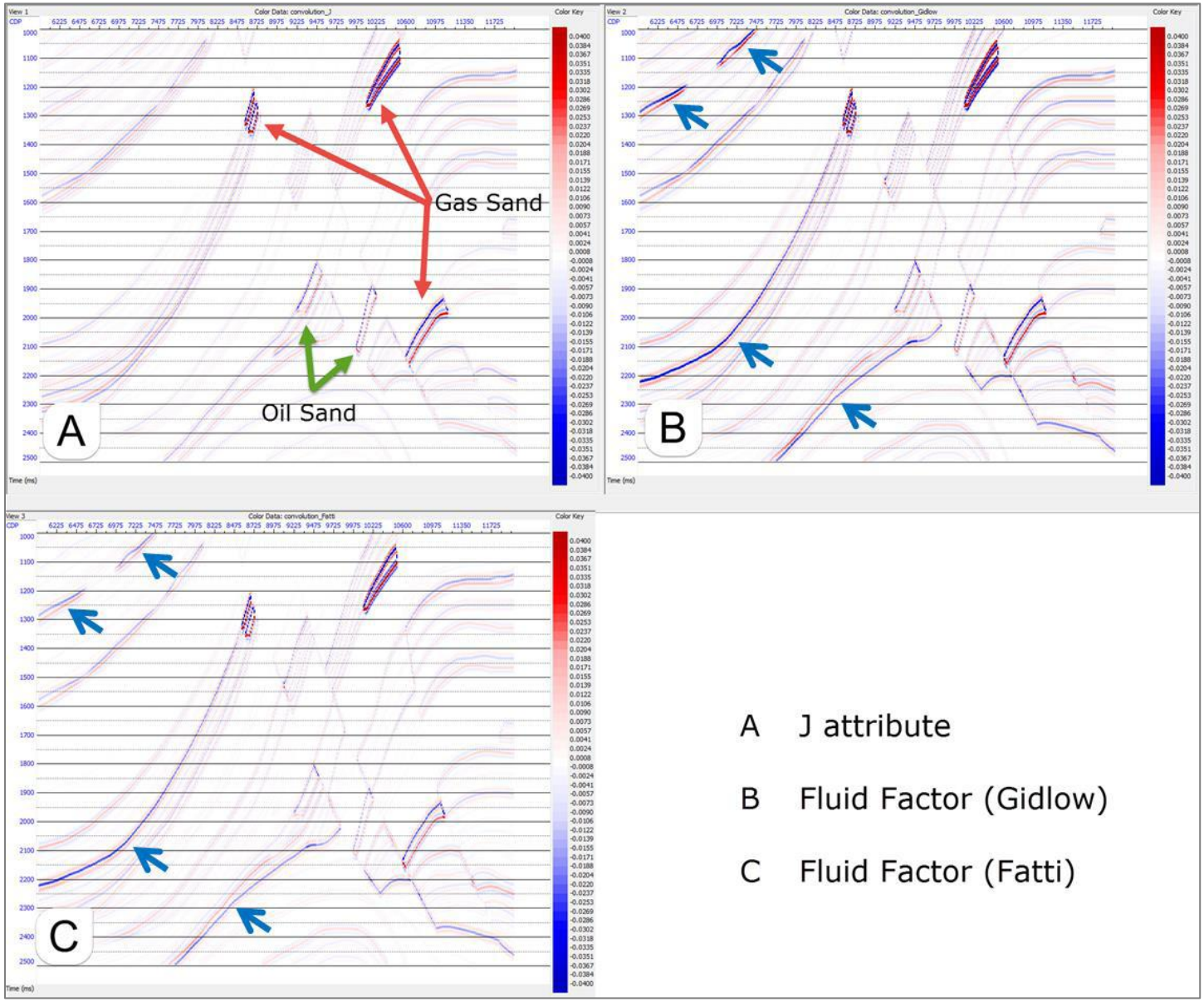


Figure 5. Attribute responses (A) J attribute; (B) Fluid factor presented by Smith and Gidlow; (C) Fluid factor presented by Fatti. Results are convolved with a 30Hz Ricker wavelet.

| | Bulk Modulus K (GPa) | Shear Modulus μ (GPa) | Bulk Density ρ (g/cm$^3$) |
|---|---|---|---|
| Shale | 10 | 1.6 | 2.5 |
| Quartz | 36.8 | 44 | 2.65 |
| Oil | 1 | 0 | 0.8 |
| Gas | 0.02 | 0 | 0.001 |
| Water | 2.8 | 0 | 1.09 |

Table 1. Rock physics parameters of some composites. Shear modulus of fluid is considered as zero.